

I. Introduction

The first element in the production chain of NuMI neutrinos is the 120 GeV primary proton beam. This beam is extracted from the Main Injector and transmitted roughly 1200 feet to an underground target hall. The chief criteria which have guided the design of this beamline have been transmission of high intensity with minimum losses and precision of targeting.

The beamline specification calls for the transmission of a 4×10^{13} proton pulse every 1.9 seconds. While generation of this intensity is not yet possible in the accelerator complex, 50% of it is achievable at present and upgrades are being planned to reach, or exceed, the specified value. At the design intensity, NuMI would use each year a number of protons comparable to that accelerated in Fermilab's entire history to this point.

There are problems associated with transmission of such an intense beam, chiefly associated with the necessity of maintaining minimal losses. The chief concerns are those of activating components and, due to the location of the beamline, contaminating groundwater. If a significant amount of beam, of order one percent, were chronically lost in any region of the line, the components in that region would be activated to a level of greater than 10 rads per hour, making maintenance problematical.

Typically groundwater contamination has not been a problem at Fermilab. This is because the water has been situated many feet below the level of beamlines and accelerators. Basically, in the time taken for any radionuclides to migrate down to the level of an aquifer, several half-lives will have passed and the activity will have been greatly reduced. However for NuMI the primary beam is transmitted to and into the aquifer region. Thus the decay time argument does not apply and the loss criteria are made much more stringent.

The criteria for targeting of the proton beam, specified in detail below, are not unprecedented. However they are nonetheless severe. The one feature which is new is the requirement to point the beam accurately at a distant location, namely the Soudan mine. The secondary hadron and neutrino beams are produced at zero degrees relative to the proton beam and thus it is imperative that the proton beam be accurately directed at Soudan at the point of targeting. Since a primary signature of neutrino oscillations is a shortage of muon neutrinos at the far detector, it is imperative to assure that no deficit arises due simply to poorly aimed beam.

II. Specifications

The specifications established for the proton beam are as follows.

- Positional precision and stability The position specification on the target is established by the physics of the experiment as 0.5 mm. The instrumentation specified will be adequate to fix the beam center within $\pm 100 \mu$ and the program Autotune will be used to maintain the position to high precision. The position stability upstream of the

target is not fixed by physics. However variation which can be corrected to the 1 mm level is required by aperture considerations.

The level of concern over positional instability, due to power supply regulation, depends on how any such instability occurs over time. If a variation happens over minutes or hours it will be correctable by tuning, while if it were to be seen as a pulse to pulse jitter correction would not be possible and the stringent specification would have to be met directly.

- Beam angle Assigning an appropriate fraction of the angle error budget, as determined from physics, to the primary beam, yields a required precision of 60 μrad at the target. The final two instrumentation stations are located 12.5 m apart, so that a 1 mm relative position error between them will lead approximately to 80 μrad . The instrumentation itself will operate with a precision of an order of magnitude better than this 1 mm value, so that the real limitation will be on the relative alignment of two detectors.
- Beam size The beam spot on target is to be round with a σ of 1 mm. A different size might be specified for a beam intensity different from the nominal 4×10^{13} protons per pulse. The specification on this size is $\pm 10\%$. It is also necessary that the beam size not change significantly over the 95.4 cm target length. Note that there is a potential contribution to the spot size due to momentum spread, but that the beam design has dispersion functions of effectively zero at the target to prevent this.
- Loss levels Losses must be minimized as they lead to air activation, component residual activity, potential equipment damage and groundwater irradiation or contamination. Loss limits in different regions along the beamline have been determined and are presented in detail in Chapter 5. The most sensitive location is that where the line traverses the interface between soil and rock. The fraction of beam loss in this, rather limited, region must be kept below a few $\times 10^{-6}$, or a handful of full intensity pulses in the average water residency time of four months. The more downstream locations, the pretarget hall and occupied parts of the carrier tunnel, with relative loss limits of 1.4×10^{-4} , are in some ways more worrisome in that smaller beam missteerings in the stub could lead to striking components there.

III. Beamline elements

- Kicker The requirements on the extraction kicker were originally presumed to be similar to those of the long-batch kicker, which used to be operational at MI52. However the MI52 first Lambertson has been found to be quite highly activated, and our simulations show that indeed the two kicker configuration which precedes it does not provide enough kick to clear the septum cleanly. Since the NuMI extraction region must transmit roughly five times as much beam as MI52 does with a likely larger transverse emittance, it has been decided to construct three, rather than two, kicker magnet modules. The three magnets will together supply 3.8 kG-m of integrated field, and achieve adequate separation at the Lambertson.

The normal operating mode will be one in which five Booster batches, each consisting of 84 18.9nsec bunches, are extracted, a single Booster batch having previously been sent to the antiproton source on the same accelerating cycle. However for periods when antiproton is not in a stacking mode it will be desired to extract six Booster batches to NuMI. This latter mode has essentially the same requirements as did six batch extraction to the Tevatron, which was effected by the MI52 long batch device. The specifications for the kicker system are given in Table 1 and a cross-sectional view of a kicker magnet is given in Figure 1. The magnets are to be located in the region downstream of quadrupole Q602.

A measured waveform from an existing kicker is shown in Figure 2. It is seen to satisfy the given specifications. However note that there is no criterion given in those specifications for fall time and that there is ringing after the pulse is completed. This feature implies that there can be no beam left in the Main Injector after NuMI extraction and thus that this kicker design is not satisfactory for any scenario in which NuMI beam is extracted first on any given cycle, with extraction to antiproton following.

Table 1 - Extraction Kicker Specifications
(Most physics specifications from MI Note #258, 1/6/00 D.E.J.)

Physical & Good Field Aperture:	81 mm H x 33 mm V elliptical shape
Kick Angle @ 120 GeV:	950 μ rad to inside of ring
Field Rise Time (1%-99%):	1.30 μ s
Field Fall Time:	N/A
Field Flattop Time:	9.78 μ s minimum(6 batches)
Flattop Integrated Field:	3.8 kG - m
During Pulse:	\pm 0.5%
Pulse to Pulse:	\pm 0.5%
Repetition Rate:	1.9 seconds
Required Charging Time:	1.5 seconds

- Extraction region The primary active elements for extraction are the three Lambertson magnets. The methodology followed for establishing beam orbits in the MI60 region, where these magnets are located, is as follows. A horizontal excursion of the circulating beam is established, primarily by offsetting several quadrupoles; the required displacements are given in Table 2. Once extraction energy has been approached and beam size has decreased, corrector magnets are used to make an additional contribution to the excursion; Table 2 includes the fields. The bumps are all constructed to be local so that the circulating beam is unaffected outside the extraction region. With the circulating beam on its 'extractable' orbit the kicker is fired and creates an extraction bump extending from location 602 through 608 and terminating in the field region of the Lambertsons.

A complication is that the strongly focusing MI lattice requires that a quadrupole, Q608, be placed between the Lambertsons. One effect is that the extracted beam passes through this magnet off-center and sees considerable quadrupole steering. This steering must be

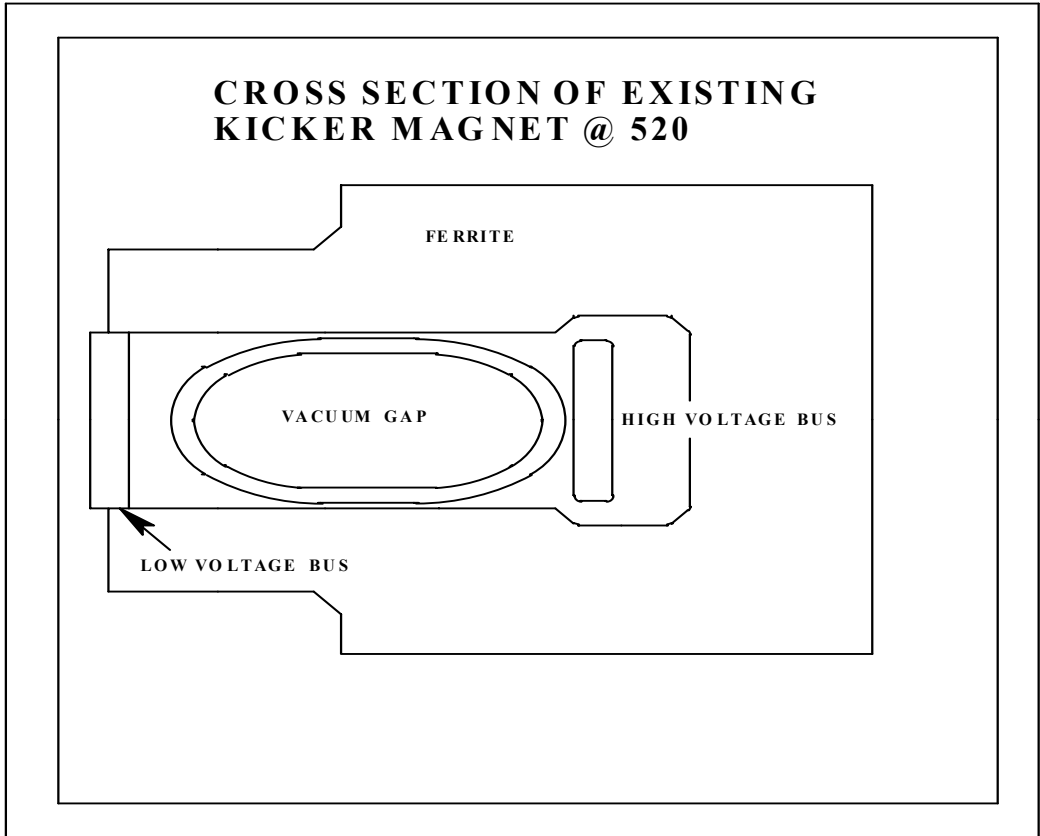


Figure 1: Kicker magnet cross section

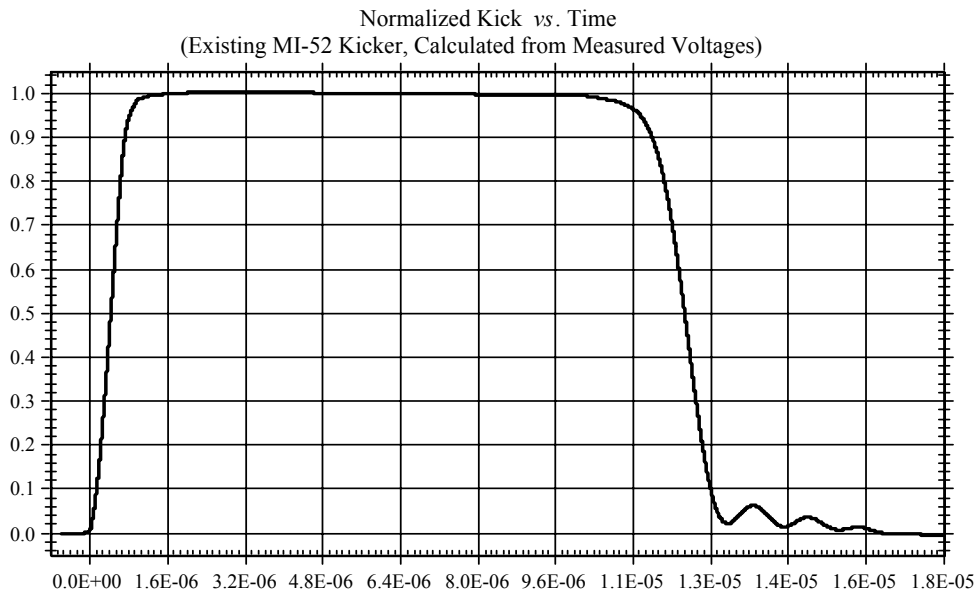


Figure 2: Measured MI52 long-batch kicker waveform

Table 2 Extraction Parameters

Quadrupole displacements: (x positive is toward the outside of the ring)

Q602: X = 3.1 mm
Q606: X = -.55 mm
Q608: X = -3.9 mm
Q610: X = -3.7 mm
Q612: X = -3.4 mm

Horizontal corrector fields at extraction:

H602: B = -.726 kG
H604: B = -.039 kG
H606: B = .208 kG
H608: B = 1.341 kG
H610: B = 1.427 kG
H612: B = 1.509 kG

Lambertson fields & septa positions:

LAM60A: B = 5.324 kG; X = 2.0 mm, Y = -1.5 mm, rotation = .145 radians
LAM60B: B = 10.734 kG; X = 2.0 mm, Y = 0, rotation = .020 radians
LAM60C: B = 10.734 kG, X = 2.0 mm, Y = 0, no rotation from vertical

counteracted by a horizontal kick from the Lambertsons and thus the first two are rolled to provide an outward deflection in what is primarily a vertical bend. A second problem is that the, primarily vertical, kick that Lambertson 1 generates makes the aperture of the quadrupole limiting on the beam which can be transmitted into the line. Due to this effect the first Lambertson is run at a reduced current. To effect extraction Lambertsons 2 and 3 must be run somewhat above their nominal value, though still within their specified current limit. Figure 3 shows the circulating and extracted orbits together with an expanded view of the 608 region. The clearances of the beam vs. septa and apertures in the extraction region are discussed in Appendix B.

Figure 4 shows the results of a tracking study through the extraction channel. The quantity plotted is the fractional beam loss through the extraction region as a function of kicker strength. The losses on the left side of the figure, for too small kick, are found to occur primarily on the septum of Lambertson 1; while those on the right, for too strong kick, occur on the Q608 aperture. The chosen strength of 3.8 kG-m is well centered in the minimal loss region.

The final extraction element is a standard MI C-magnet, installed as a pure vertical bend and positioned as far upstream as possible given physical constraints.

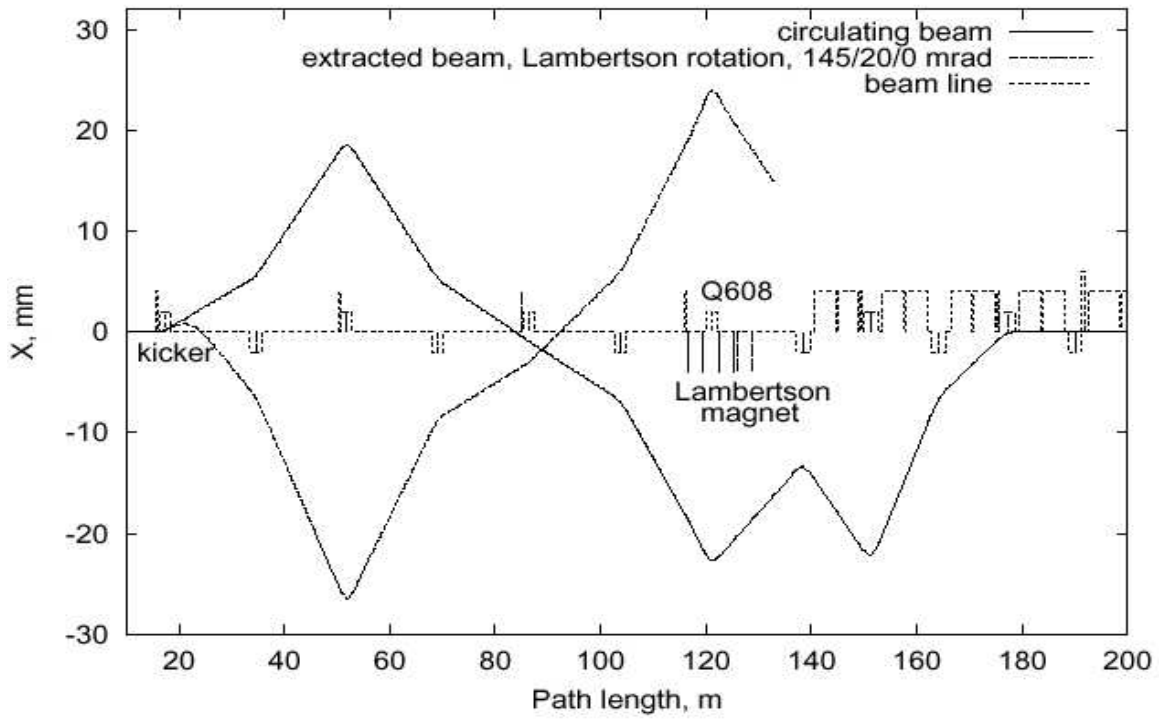


Figure 3a. Circulating and extracted beam orbits in the MI60 region

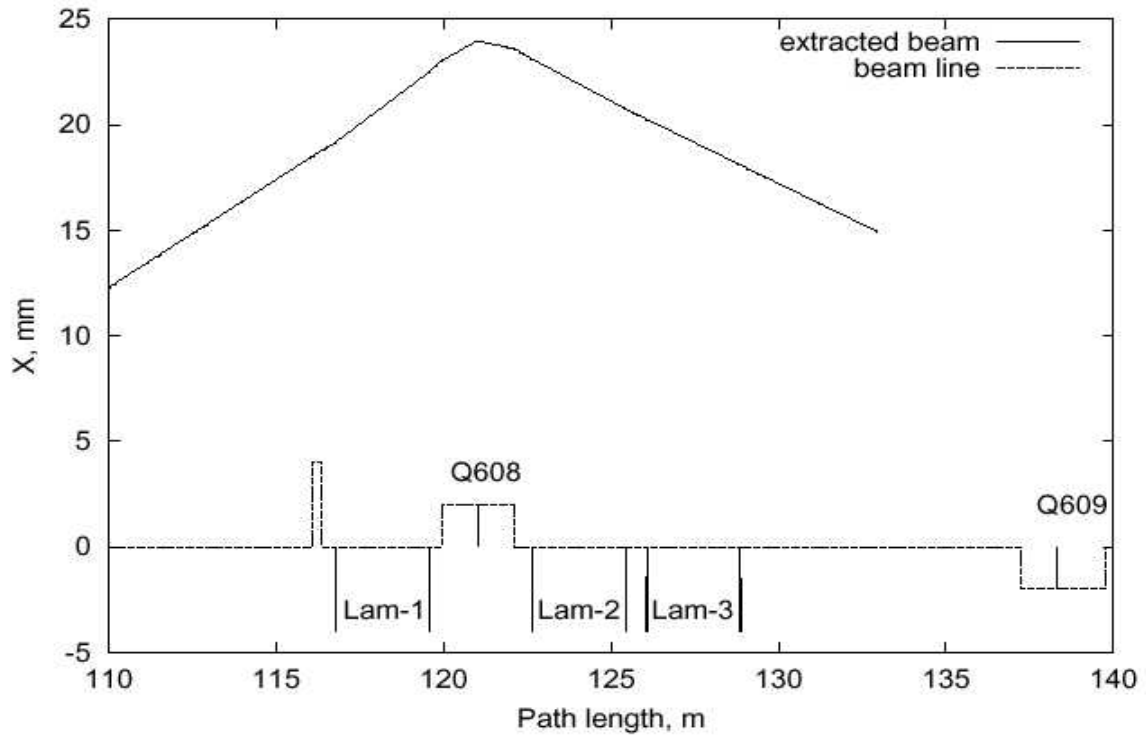


Figure 3b. Extracted beam orbit through Lambertsons

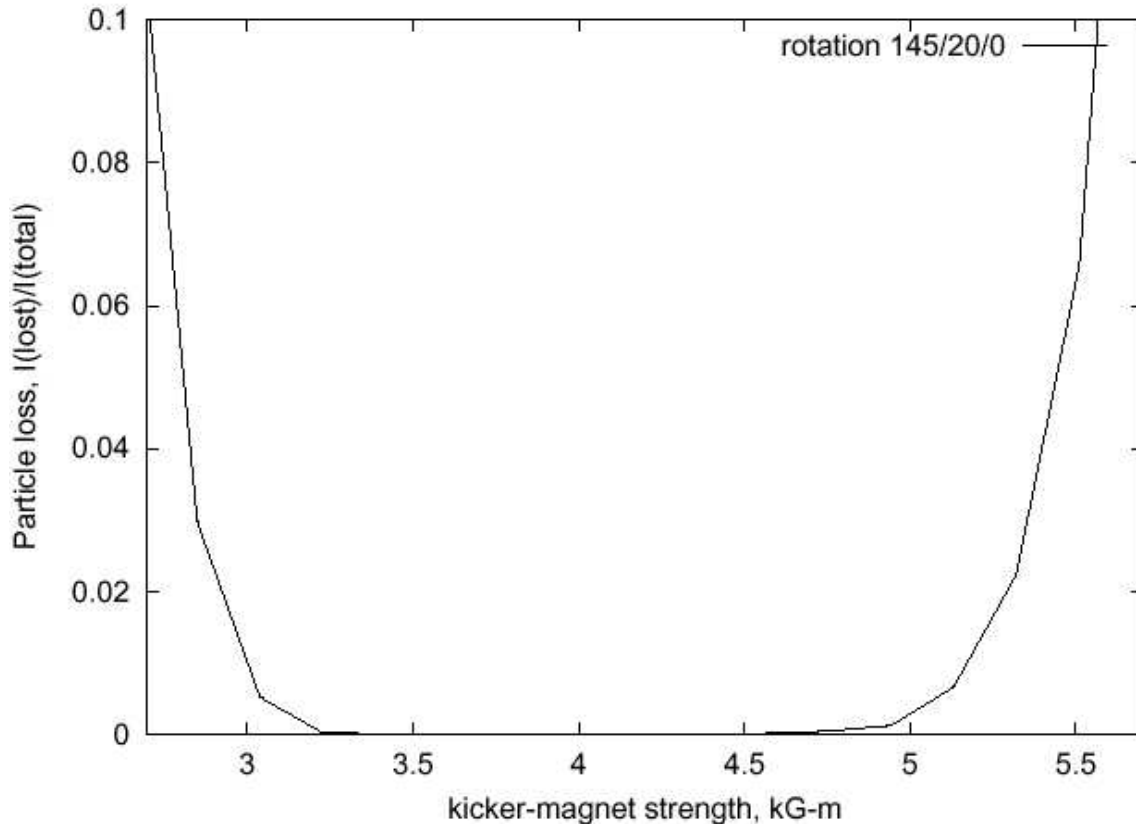


Figure 4. Extraction losses vs. kicker strength

- Beam transport and targeting The beam transport consists of three bend regions together with quadrupole focusing in the straight sections connecting them. The quadrupole layout and design principles are discussed in detail in TM-2174 (May 28, 2002; John Johnstone, author). Table 3 presents all of the elements of the line.

There are 21 quadrupoles in total. The first 15 provide a match with the MI optics, a suitably focused transfer through the MI tunnel and a well behaved passage through the carrier region where no components are installed. The last 6 form the final focus optics to obtain the desired beam size at the target and also to eliminate vertical and insofar as possible horizontal dispersion there. The final focus segment is optically flexible and can comfortably accommodate tuning to different beam sizes and shapes.

- Layout Figure 5a shows the extraction region (partially obscured) and the first beamline bend. It is seen that the NuMI line in this region fits comfortably between the MI below and the Recycler ring above. The bend in this region comes from a string of six EPB dipoles, powered in series to the design field of 15.0 kG but rolled at five separate angles. In the horizontal plane the deflection is such as to accomplish most of the horizontal bend required to hit Soudan, a small final bend in pretarget accomplishing the remainder. In the vertical the goal is to have the beam exit this region level, or nearly so, so as to avoid generating interferences with existing equipment. The actual pitch angle

Table 3 Components of the Primary Proton Line

<u>Element</u>	<u>Number</u>	<u>Purpose/Comment</u>
Dipoles:		
EPB	6	Transport in MI60 region
B2	10	Downbend in NuMI stub, upbend in pretarget
Eartley	2	Trim in MI60 (provides a strong horizontal corrector in this area), 1 horizontal bend in pretarget
Quadrupoles:		
3Q120	17	Transport and targeting
3Q60	4	Transport
Trims:		
Horizontal	10	MI IDH correctors, two to have aperture increased from 1.0" to 1.5"
Vertical	9	MI IDH correctors rolled 90 degrees, two to have aperture increased from 1.0" to 1.5"
Beam instrumentation:		
Horizontal BPMs	13	Two nearest target to have double resolution
Vertical BPMs	11	Two nearest target to have double resolution
Multiwires	10	Two nearest target have .5 mm wire spacing, others have 1 mm wire spacing
Toroids	2	Measure intensity in line with some redundancy
Total loss monitors	4	Integrate losses over major beamline sections
Sealed loss monitors	35	Localize any loss points

achieved is $-.27$ milliradians. Figure 5b shows the NuMI line passing above the A150 line in the MI tunnel.

To be directed toward Soudan vertically it is necessary to bend the protons at a pitch of -58 milliradians. What is actually done is to bend by -156 milliradians, the goal having been from a civil construction standpoint to descend below clay soil into bedrock as soon as possible, and then to bend back $+98$ milliradians to set the final pitch. The downbend occurs in a region known as the northeast extraction enclosure (NuMI stub), basically an alcove-like extension of the MI60 straight section. This region and the beamline in it are pictured in Figure 5c. The downbend is accomplished by a string of six Main Ring B2 magnets, rolled by 90 degrees. The bend field of 17.1 kG is safely below the design value of 17.8 kG. If left uncompensated this major downbend would generate a significant vertical dispersion. A major accomplishment of the optics design is that dispersions are kept reasonable throughout.

Figure 5d shows the downstream end of the beamline, the upbend and the focusing region which takes beam to the target. Also present here is the small horizontal bend ($.40$ milliradians) necessary to hit the target while simultaneously having beam directed

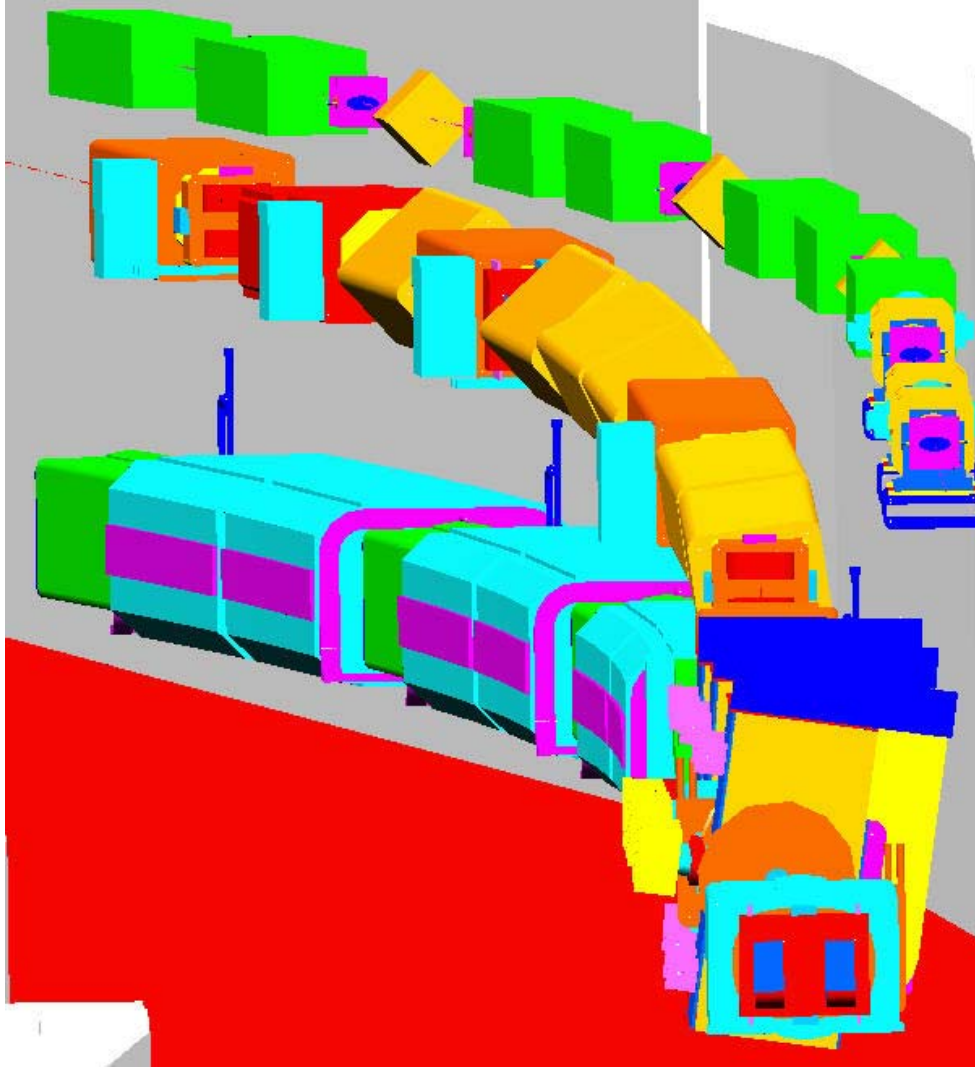


Figure 5a. The MI60 region, of the NuMI beamline. The MI ring is on the bottom, the Recycler ring is on the top and the NuMI line is between.

toward Soudan. This is effected by a 5' long "Eartley" dipole. The major upbend here is again achieved by rolled B2 dipoles, in this case running at 16.1 kG.

A feature to note, which is only partially indicated by the figure, is that there is a considerable drift space, nearly 23 meters in total, from the last magnet to the target. Some of this space is inside the shielding pile and is reserved for an upstream move of the target if the need ever arises to change the secondary beam focus and raise the neutrino energy. Also inside the shielding is a graphite collimator, or baffle, whose purpose is to protect the target water system and the focusing horns from errant primary beam.

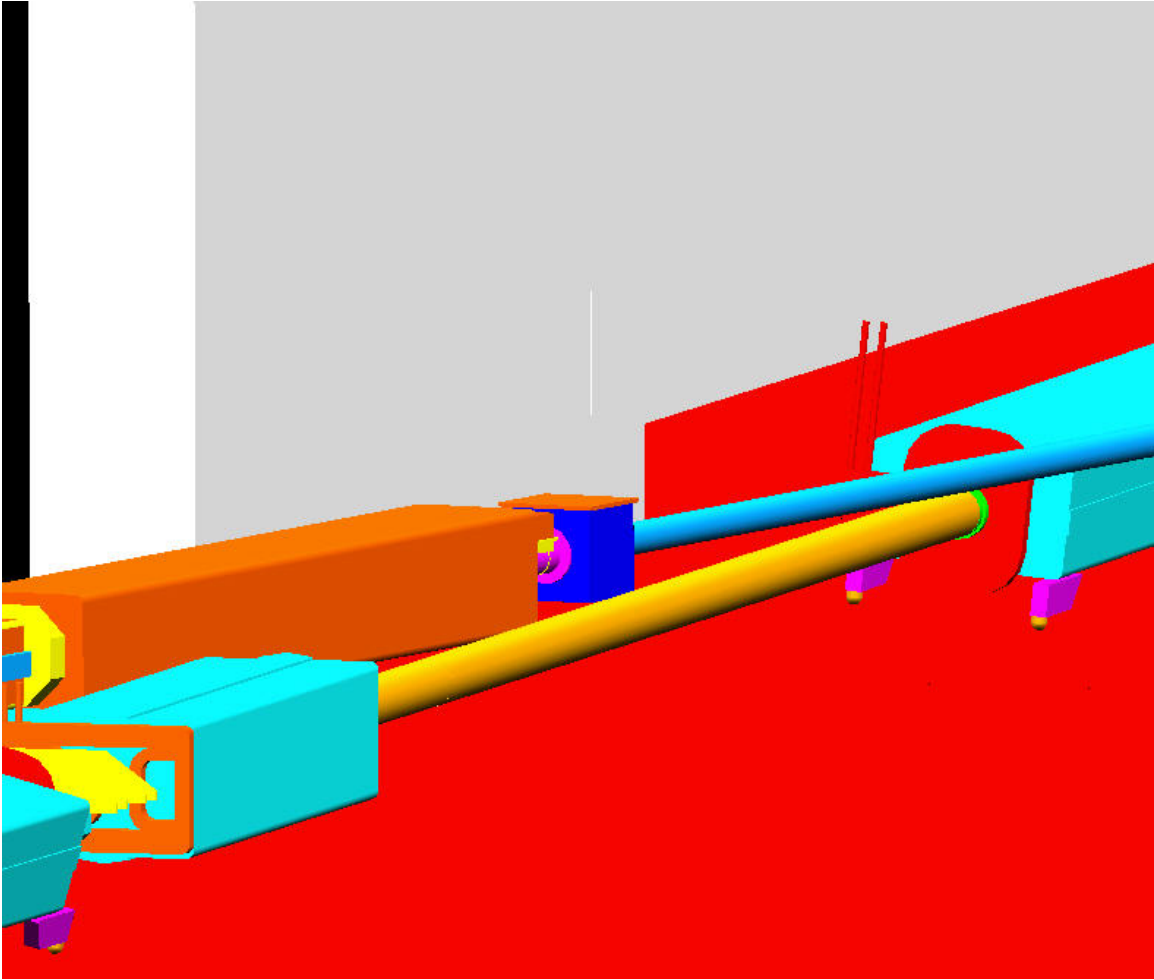


Figure 5b. View of the region where the NuMI beamline passes above the A150 line

Some of the drift space (~14.25 meters in length) outside the shielding is available for instrumentation. At the upstream end of this space is a complete instrumentation station, with horizontal and vertical BPMs and a multiwire profile monitor. Each of these monitors is specified to have double the accuracy of the ones in the transport region. Similar instrumentation is placed at the downstream end of the free space. Such good instrumentation at two separate locations allows the proton beam direction on target to be measured quite accurately, assuring that the protons, and thus the secondary mesons and neutrinos, are directed accurately toward Soudan. The target profile monitor is also crucial for ascertaining the beam spot size near the target. The beam will begin to miss the target in the horizontal direction if its width becomes significantly larger than the specified 1 mm sigma.

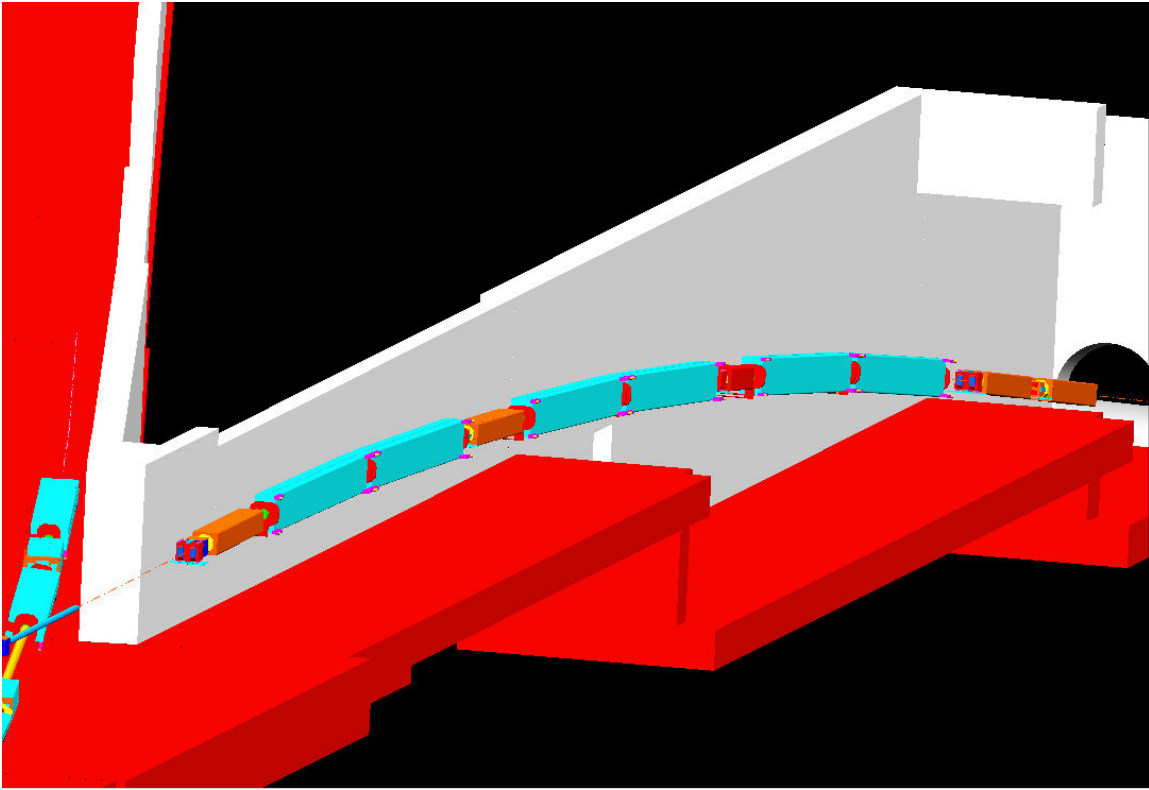


Figure 5c. View of the NuMI beamline as it traverses the MI northeast extraction enclosure (NuMI stub)

Figure 5d. *IN PREPARATION* View of the NuMI beamline in the pretarget region

IV. Instrumentation

EDITORIAL NOTE: This section will be developed further to detail instrumentation use in maintaining fractional beam loss levels at $<10^{-4}$.

A. Overview

The instrumentation of this beamline is designed to serve two purposes. The first is to assure that the beam is accurately on target and is directed accurately toward the far detector. The pointing requirement on the primary beam, $60\mu\text{rad}$ as noted above, is about as stringent as those requirements of other fixed target experiments. The second purpose of the instrumentation is to aid in the effort to keep any losses at an absolutely minimum level. It will do this by providing: position information to assure that the beam is in the center of its vacuum chamber, profiles to allow unexpected beam tails and halo to be observed, sensitive loss measurements to allow beam problems to be immediately addressed and intensity measurements in the ring and in the line to serve redundantly with the loss monitors in the case of large losses.

All of the instruments specified are of types which already exist in either the Main Injector complex, the Tevatron or the Switchyard. However NuMI will utilize unprecedented beam intensities at this energy. Thus a particular requirement placed upon

the instruments is that they be functional over a wide range (at least two orders of magnitude) of intensity. This will allow all beam tuning to be done at low intensities, high intensity only being run after all beam properties are declared nominal.

B. Profile Monitors

All profile monitors will be of the type known as multiwires. The operational principle is that of secondary electron emission from wires which are placed in the beam. There are neither gas nor gas containment windows which would provide additional material in the beam beyond the wires themselves, which intercept 10% of the beam and scatter 10^{-4} of it. There are 10 of these devices, each having 48 horizontal and 48 vertical wires. The wire spacing is 1mm for the upstream eight units and .5mm for the last two, which are used in targeting the beam.

All units will have motion control into and out of the beam as directed through the control system. A new design is under development which will allow the motion to take place while beam is running, no significant material ever intercepting it.

The amplifiers which produce the readback signals will have gains variable in steps over two orders of magnitude, to facilitate the operation at different beam intensities. Typical intensity profile readouts from a series of multiwires are seen in Figure 6. Changing amplitude and dispersion functions affect profile widths significantly.

C. Position/intensity monitors

There are specified 24 position/intensity monitors, 13 horizontal and 11 vertical. These intercept no beam and will provide position information during normal operation. The position specification for the upstream ones is a fairly standard .2 mm RMS. For the last four, those used in targeting, .10 mm RMS is specified; this is more challenging but comparable to what has been achieved by the collision point position monitors in the Tevatron collider. All units have intensity, as well as position, readouts.

As is the case for the profile monitors, there will be switchable gain amplifiers to facilitate running over a wide range of intensities. It will be particularly important to confirm in this case that a gain change does not lead to an apparent position change. It is being considered whether these units, or perhaps only the targeting ones, should have high bandwidth readout which allows the position to be measured multiple times in the 10 μ sec spill time.

D. Toroid intensity monitors

Toroids are often used for intensity measurements as they provide better accuracy than BPMs, are stable, reliable and subject to absolute calibrations. There is a toroid in the MI ring - observation of the change in ring intensity obtained from it over NuMI extraction provides a measure of the beam delivered. There will be two similar devices in the NuMI line to assure within a few percent accuracy that all beam removed from the MI indeed enters the line and arrives in the vicinity of the target.

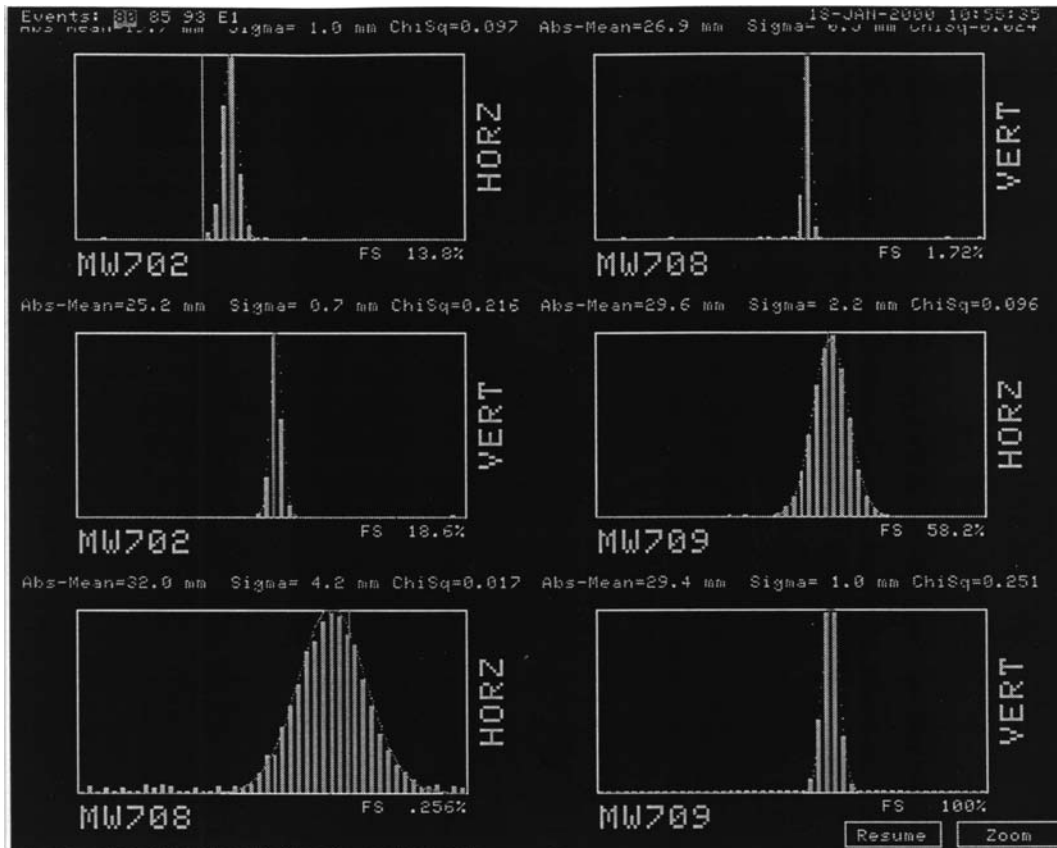


Figure 6: Horizontal and vertical profiles for a series of three multiwire monitors

E. Loss monitors

Two types of loss monitors will be used, both copies of existing equipment. First there are standard sealed units, 35 in number. These are placed at every location along the beamline where the aperture becomes smaller, as well as at every second magnet in bend strings. A photograph of a sealed unit, indicating the dimensions, is shown as Figure 7. The second type is known as total loss monitors. The present plans are for three of these - two in the carrier tunnel covering separately soil and rock regions, and one covering the length of the pretarget hall. The total loss monitors are sensitive in a calibrated fashion to any and all losses over the region covered.

The electronics to be used for the loss monitors will be like that developed for the Main Injector beamlines, where several decades of linearity have been demonstrated, see Figure 8. These monitors will likely provide the first warning of many types of beam delivery problems. The intensity monitors will see losses at the level of a few percent, but the loss monitors will be several orders of magnitude more sensitive and will provide a primary means of troubleshooting.



Figure 7: A standard sealed unit loss monitor

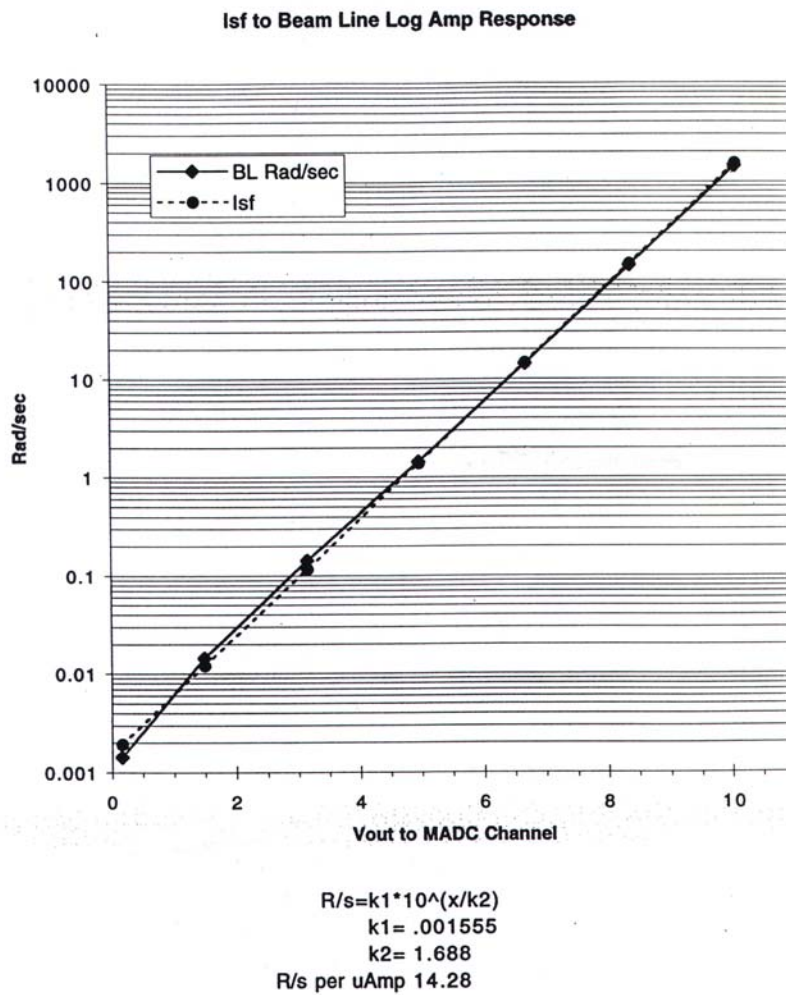


Figure 8: Measurement of the range and linearity of a standard loss monitor

Appendix A. Beamline Sensitivity Effects

The sensitivity of the beamline to various off-nominal conditions has been investigated. Specifically addressed are the sensitivity of focus and of trajectory.

Focusing sensitivity The sensitivity of the optics to different error sources has been studied in simulations. Assigning random gradient errors of $\sigma(\Delta B'/B') = 25 \times 10^{-4}$ to the 21 quadrupoles in the line, Figure A1 shows the beam sizes resulting from 20 random generator seeds. The changes in beam σ 's are demonstrated to be less than ≈ 0.1 mm. At the target the maximum changes in beam size are on the order of 0.05 mm, within the specification.

Optical errors also arise from discrepancies between the assumed and actual MI lattice functions. Figure A2 shows the β -envelopes (proportional to squares of beam sizes) that result from $\pm 10\%$ variations in the nominal β_x and β_y values. The maximum β 's are sufficiently well-behaved that no aperture problems arise, and the small residual mismatch at the target can be corrected with 4 or 6 final-focus quadrupoles.

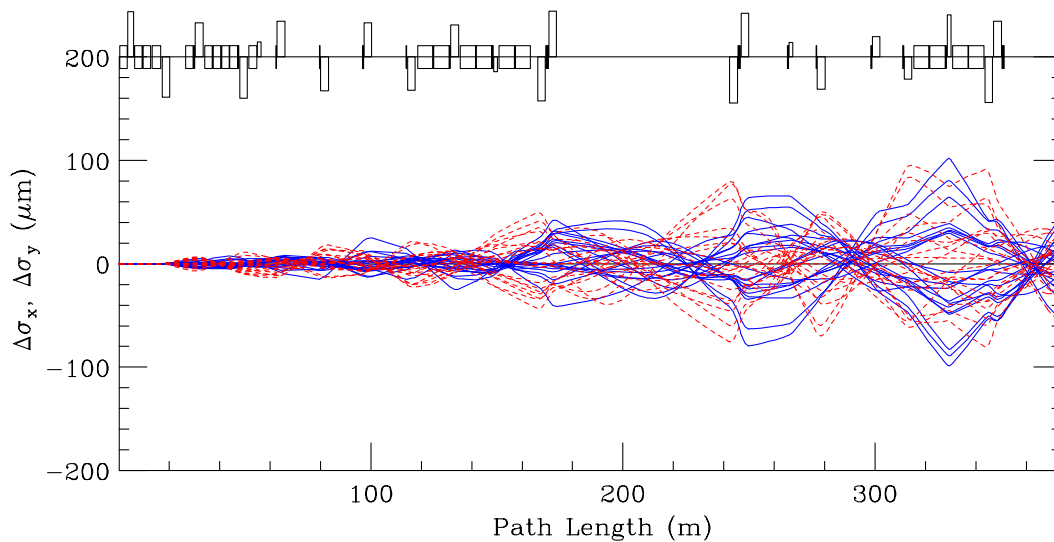


Figure A1. Beam size variation resulting from random gradient errors

Trajectory sensitivity and correction Most focusing elements in the line have associated position monitors. Orbit correction is an issue which, of course, must be addressed by any beamline, but for the ultra-clean transport requirements of NuMI it is critical that precise position control be available throughout.

Correction of central trajectory errors has been simulated with dipole field errors and random misalignments assigned to the beamline elements (including position monitors). Suitable error values are 0.25 mm for positions and 10^{-3} for magnetic field fractions. Figure A3 shows the deviations from the central trajectory arising from 20 random error seeds. The uncorrected offsets in the line are $\Delta x(\text{rms}) = 2.63$ mm, $\Delta x(\text{max}) = 13.03$ mm,

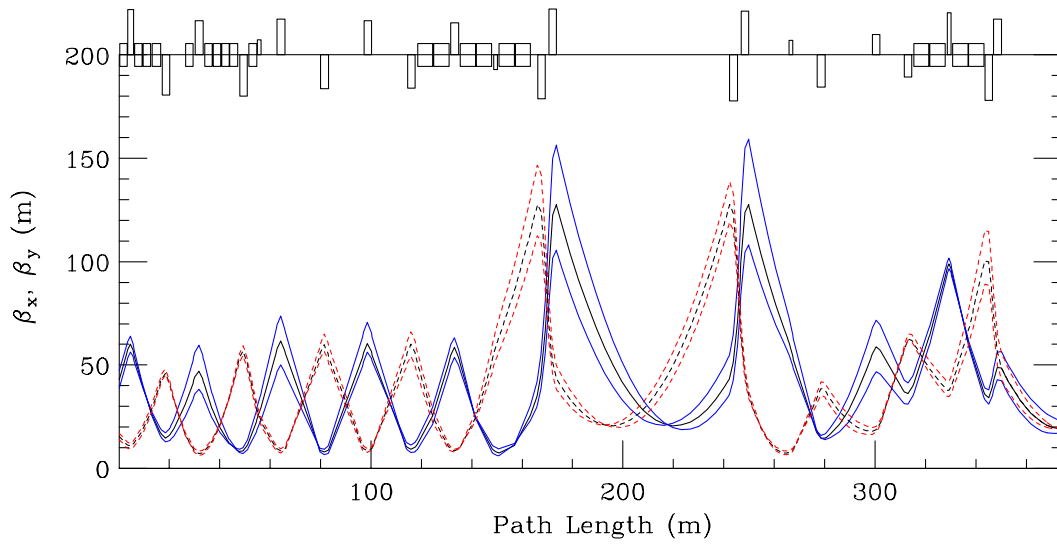


Figure A2. β -waves due to $\pm 10\%$ injection optic errors

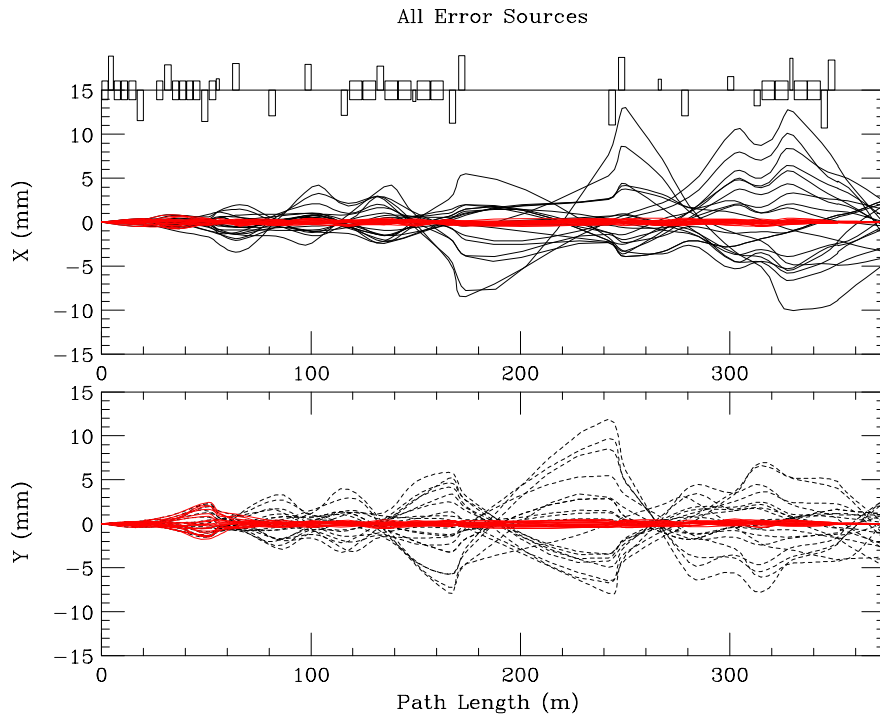


Figure A3. Uncorrected and corrected trajectories with random misalignments and dipole field errors

and $\Delta y(\text{rms}) = 2.33 \text{ mm}$, $\Delta y(\text{max}) = 11.90 \text{ mm}$. There is some concern, however, that the NuMI positioning errors will be greater than .25 mm, at least originally, in which case the trajectory errors will scale accordingly.

The orbits from the above analysis as corrected by the trim magnets are shown in red in the figure. They are, again, within specification, though for the vertical they require more

trim strength than is available in MI vertical correctors. It is for this reason that rolled horizontal correctors are specified for the vertical plane.

The sensitivity of the line to possible dipole mispowering is a subject of considerable interest and is now presented in greater detail. Figure A4a shows the situation for the horizontal plane and Figure A4b for the vertical. What is plotted is, for each bend supply, the effect on downstream beam positions of a .1% power supply drift of the peak current. Comparing with the specification of <0.5 mm for target position (the target is located at station 356 meters), it is seen that at least the major up and down bends will need regulation considerably greater than that used in making the figure. Taking into account the specification for stability along the beamline, the EPB string also requires more regulation. The power supply stability specifications resulting from this analysis are presented in the 1.1.3 section of this Handbook. They are accomplished via techniques in use elsewhere in the laboratory.

Horizontal Beam Sensitivity to Nominal PS Drifts

September 30, 2002

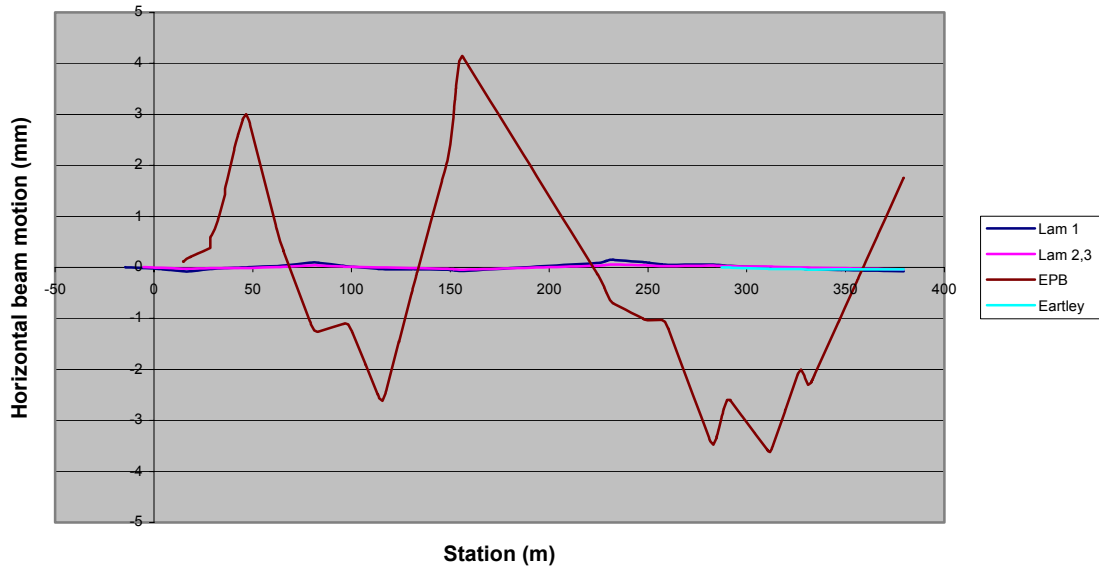


Figure A4a. Sensitivity in the horizontal plane to dipole power supply variations

Vertical Beam Sensitivity to Nominal PS Drifts

September 30, 2002

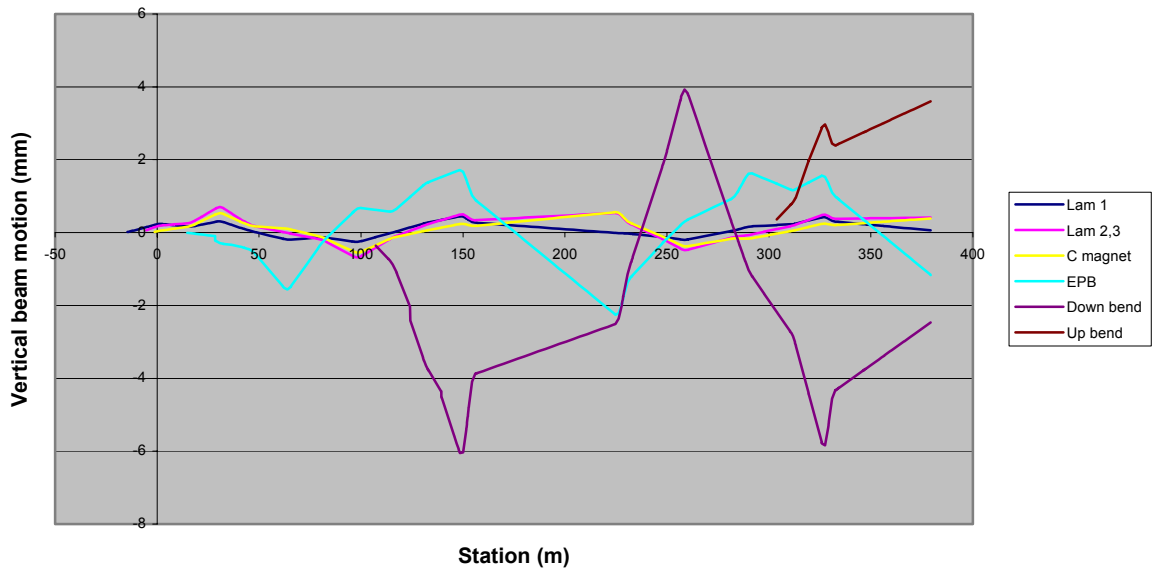


Figure A4b. Sensitivity in the vertical plane to dipole power supply variations

Appendix B. Aperture Considerations

Figure B1 shows the amplitude (root β) and dispersion (η) functions over the entire line. The beam size peaks at stations 150 m and 225 m are at the upstream and downstream ends of the unoccupied carrier region. Putting relatively large sizes at these quadrupoles allows the sizes upstream and downstream of them to be appropriately small. To prevent the running of any quadrupole at a current value which would endanger it, a limit of 16.0 T/m has been placed on the gradients.

Figure B2a shows the clearances vs. beam size over the entire line and Figure B2b shows an expanded view of the same in the Lambertson region. Considerable effort has gone into having a design for which this plot demonstrates adequate clearance over the length of the entire beamline, and several of the plot's features are worthy of detailed discussion. The aperture, or preferably clearance, shown for each element is the actual half-aperture of the device minus any sagitta in that device.

What is shown as clearance for the Lambertsons, and for MI quadrupole 608 which lies between Lambertsons 1 and 2, is worthy of special comment. The alignment of each of these magnets is determined by the path of the circulating MI beam, not the extracted beam. Thus the effective clearance is the distance from the beam center to the nearest aperture restriction, which for all Lambertsons is the septum. Note that the tighter clearance is in the horizontal plane and that the first two Lambertsons are rolled so that the horizontal distance to the septum is dependent on the height of the beam. Secondly,

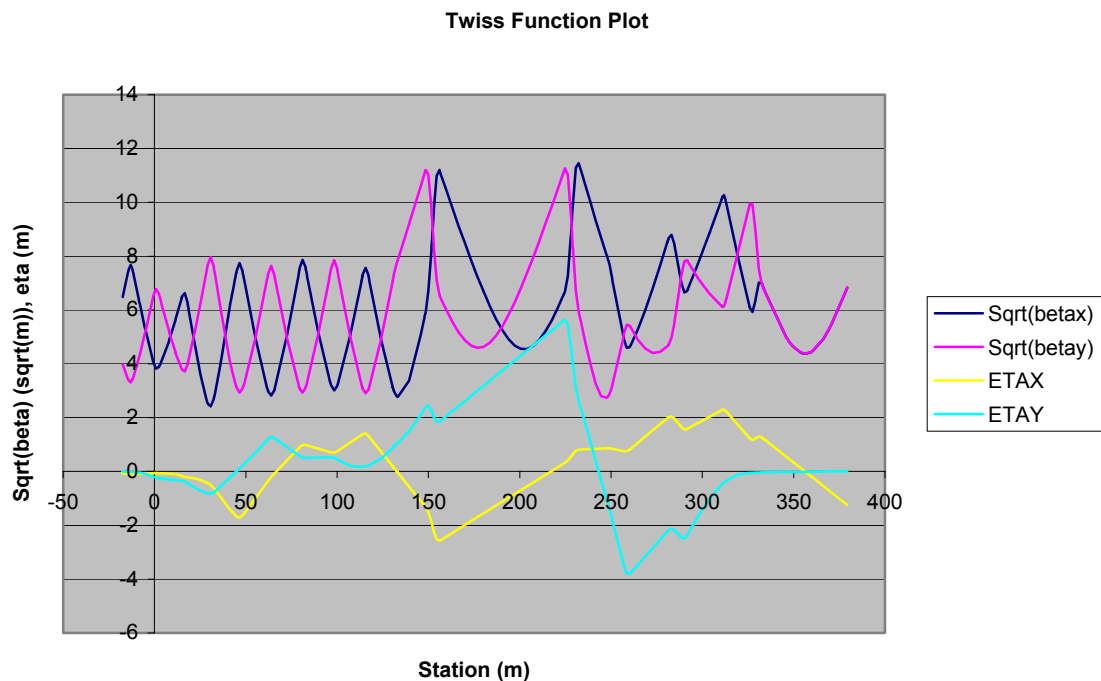


Figure B1. Amplitude and dispersion plots over the entire beamline. The target station value is 356 meters.

Maximal Beam Sizes vs Clearances

09/27/02

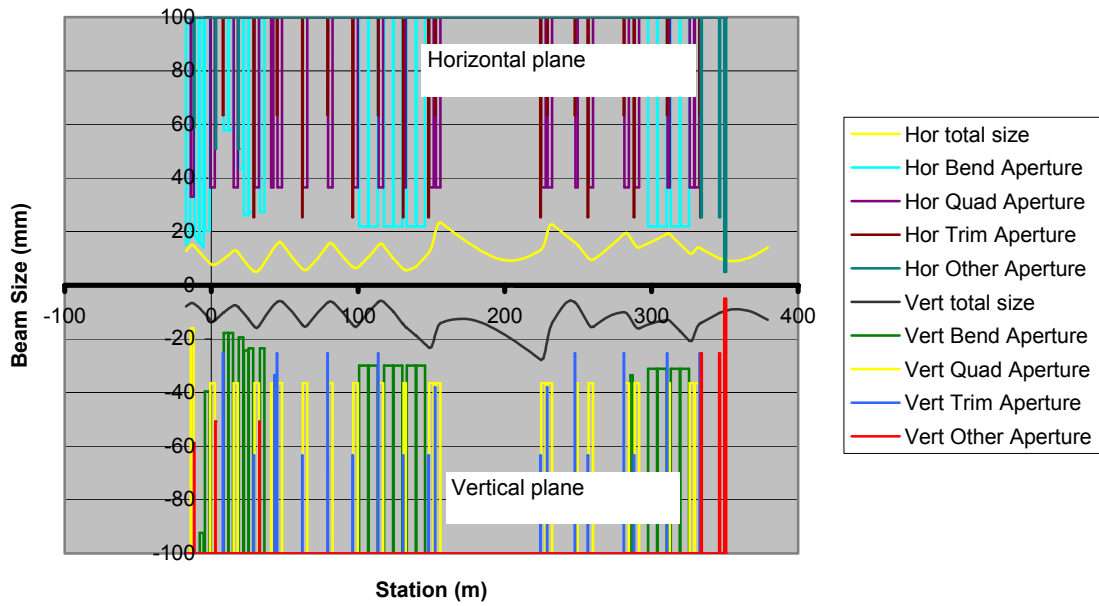


Figure B2a. Beam and aperture clearance plot over the entire beamline

Clearances in Lambertson Region

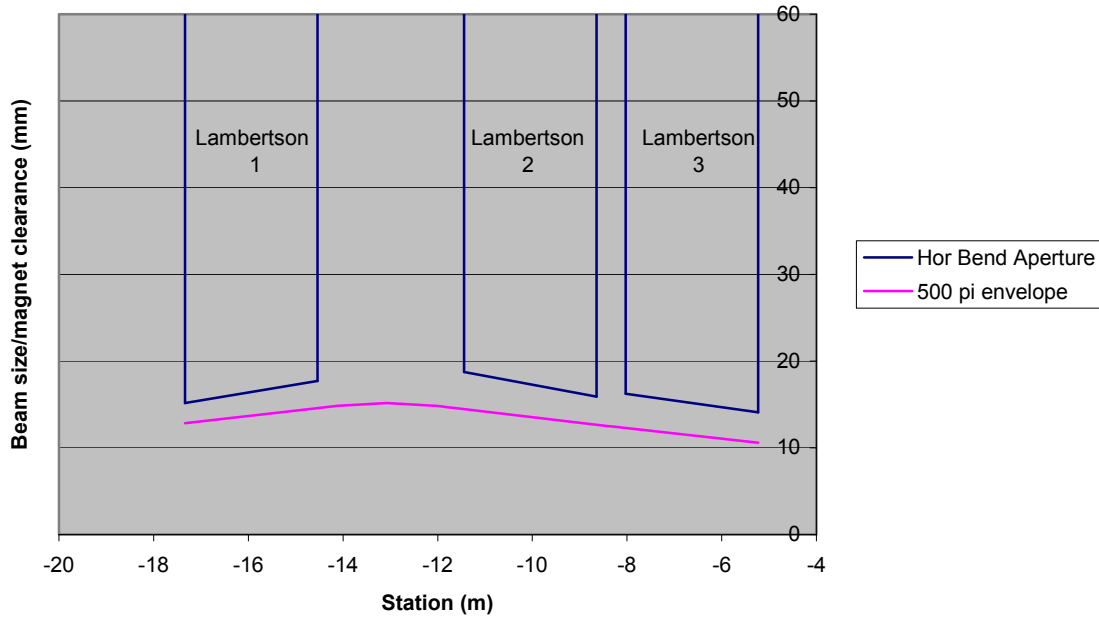


Figure B2b. Beam and aperture clearance plot in extraction region

since the magnets are aligned along the circulating beam direction, the extracted beam is not traveling parallel to the septum face. Additionally, the beam size can change over the length of one element, again affecting the effective clearance. All of these effects have been accounted for in making the plots, which have what appears as angled magnet apertures but which really are angled beam trajectories. Similarly for the case of Q608, what are plotted as clearances are horizontal and vertical distances to the edge of a star shaped vacuum chamber.

As to the beam size plotted, what is shown corresponds to the MI *admittance*, i.e. the largest beam size which the accelerator could possibly spew forth. The figure indicates that the beamline can indeed transmit this worst possible beam. Note also that the desired criteria at the target are met – the beam size has a minimum in both planes at that location.

- At station 350 m is an aperture through which the beam apparently does not fit. This aperture is that of the horn protection baffle. The worst case beam, as is plotted here, will indeed not fit through this baffle. However the more nominal beam size, as is expected in general, does fit.